Transactions, SMiRT-23
Manchester, United Kingdom - August 10-14, 2015
Division X

LATERAL LOAD CAPACITY OF STEEL PLATE COMPOSITE WALL STRUCTURES

Peter Booth[1], Amit H. Varma[2] Jungil Seo[3]

[1] PhD Candidate, Purdue University, West Lafayette, IN, USA
[2] Professor, Purdue University, West Lafayette, IN, USA
[3] Research Engineer, Purdue University, West Lafayette, IN, USA

ABSTRACT

This paper presents results from an analytical study of the lateral load behaviour and capacity of structures consisting of several connected steel-plate composite (SC) walls. When multiple SC walls are assembled into a structural system, such as a flanged shear wall where perpendicular walls are connected to both ends of a shear wall, or a core wall configuration where four walls are connected together into a rectangular shape, the shear strengths of the individual walls are influenced by the overall response of the system. The flange walls function as boundary elements by resolving diagonal compression stresses in the shear wall concrete as vertical tension in the flange wall. This mechanism can result in higher concrete stresses when the wall is at peak strength leading to a higher ultimate strength of the wall system. A method is described for calculating the shear strength of SC walls with boundary elements using composite shell theory. The calculated strengths are compared to the results of experimental tests of flanged shear walls in the literature. A detailed 3-D nonlinear inelastic finite element analysis is then conducted of an SC wall structure that is square in plan. The analysis considers two key parameters: the overall structure aspect ratio (h/L), and the reinforcement ratio of the SC walls (ρ). The governing failure mode of the core wall structure is either controlled by shear failure of the web walls or flexural failure of the whole system depending primarily on the overall structure aspect ratio. The ultimate strengths from the SC wall analysis are then compared to the calculated shear strength and a rigid-plastic fibre model calculation of flexural strength.

INTRODUCTION

Steel-plate composite (SC) walls are used in a number of new power plant designs that utilize modular composite construction. The walls are constructed from prefabricated steel structural modules that are erected and connected together at the construction site to form various parts of the containment internal structure. SC walls are constructed with steel plates on the surfaces (ranging between 0.25 and 1.5 inches thick) that are connected and braced to each other with transverse steel tie members welded to the interior faces of the steel plates. The walls are filled with concrete once they have been set in their final locations and composite action is generated between the concrete infill and steel plates with shear connectors. SC wall thicknesses can vary anywhere from 12 to 60 inches depending on application.

Modular SC structural systems are usually made up of interconnected walls that provide lateral strength and gravity support for the systems in the power plant structure. In nuclear power plants, SC modules may be used for the containment internal structures and also for the external shield building such as in the Westinghouse Electric Co. AP1000 plant design (Cummins, 2001). SC structural systems are also the subject of current research as core wall structures for multi-story building structures.

The in-plane lateral behavior of an SC wall is a function of numerous properties such as the: (i) section properties of the wall, (ii) the size of the wall, (iii) the height-to-width aspect ratio (h_w/l_w), (iv) and the boundary conditions. This paper studies the in-plane shear behaviour of SC walls with boundary elements and provides a method for calculating the in-plane shear strength based on composite shell theory. The

prediction of shear strength is compared with results from previous experimental tests in the literature of SC flanged walls. A benchmarked finite element approach using Abaqus CAE (Simulia, 2013) is used to model an SC wall structure that is square in plan, and the ultimate strength of the structure is compared to the shear strength prediction. As the aspect ratio of the structure is increased, the ultimate strength of the structure becomes flexure critical. A rigid-plastic fibre model calculation is also described for predicting the flexural strength of the structure.

IN-PLANE SHEAR STRENGTH

The in-plane response of SC shear walls with boundary elements is influenced by two conditions that do not occur in shear walls without boundary elements. Walls without boundary elements (such as pier walls) must resist all of the in-plane shear and in-plane flexure. This places a higher demand on the wall and may result in lower lateral strengths. In contrast, when overturning flexure is subjected to a wall with boundary elements, the vertical flexural stresses are distributed primarily to the boundary elements. Also, walls with boundary elements are capable of developing higher concrete stresses at the point of ultimate strength since additional arch action can be developed in the wall. For this to occur, diagonal concrete compression in the wall is resisted along the perimeter of the panel and resolved as vertical tension in the boundary element on the tension side of the wall. If concrete arch action occurs, then the wall is capable of developing additional in-plane shear capacity even after the steel plates have yielded. The reserve strength is then dependant on how much additional force can be resisted by the concrete in diagonal compression.

The in-plane shear response of a shear wall with boundary elements can be divided into two phases: The first, considers monotonically applied shear force up the point when the steel plates reach yield, and the second phase considers the additional shear resisted by the concrete in diagonal compression up to the point of ultimate failure of the wall. A method is presented for calculating the upper bound shear strength, V_{ub}, that equals the sum of the calculated shear force required to reach yield, V_y, plus an incremental shear, ΔV, that takes into account the strength of the concrete due to arch action:

$$V_{ub} = V_y + \Delta V \qquad \text{(Equation 1)}$$

Composite Shell Model

An approach has been previously developed by Varma et al. (2014) and Ozaki et al. (2004) for predicting the yield point, V_y, of an SC wall subjected to in-plane shear using composite shell theory. This calculation uses a plane stress elastic composite shell model and assumes that the element is in a state of pure shear. An orthotropic concrete constitutive model is used where the concrete is considered fully cracked in the direction of maximum principal strain (the 1-direction in Figure 1) and the steel is elastic isotropic. A simplified and approximate equation (described in detail in Varma et al., 2011) based on this approach is codified in AISC N690-12s1 for the purpose of design calculations and shown in the following three equations:

$$V_y = \kappa \cdot A_s \cdot F_y \qquad \text{(Equation 2)}$$

$$\kappa = 1.11 - 5.16 \cdot \bar{\rho} \le 1.0 \qquad \text{(Equation 3)}$$

$$\bar{\rho} = \frac{1}{31.6} \cdot \frac{A_s \cdot F_y}{A_c \sqrt{f_c'}} \qquad \text{(Equation 4)}$$

In these equations, the wall yield strength, V_y, is equal to the steel plate area, A_s, on the section of critical shear multiplied by the steel yield strength, F_y and then multiplied by a coefficient, κ, that accounts for normalized reinforcement ratio, $\bar{\rho}$, steel yield strength, and concrete compressive strength, f'_c. These equations are calibrated for a range of reinforcement ratios ($2t_p/t_{sc}$) typically encountered in safety-related nuclear structures between 1.5% and 5% where t_p is the steel plate thickness and t_{sc} is the wall thickness.

Upper Bound In-plane Shear Strength

When the applied shear force increases beyond the point of steel yield, the condition of equilibrium on the composite shell element can no longer occur since the steel plates are no longer able to resist additional load. At this point, additional diagonal concrete compressive stresses in the shear wall react directly with the connected boundary elements around the perimeter. If it is assumed that the wall-boundary element connection and the boundary elements themselves are sufficiently strong, then the full strength of the concrete in the shear wall can be developed. It is then assumed that the additional incremental shear strength, ΔV, is a function of the reserve strength in the concrete infill. In order to calculate this strength, the diagonal concrete compressive stress occurring when the applied shear is equal to V_y must be determined. This stress, f_{cy}, can be calculated using the composite shell theory assumptions described previously and is shown in Figure 1(b) and equal to:

$$f_{cy} = \frac{E'_c \cdot S_{xy} \cdot (\nu_s + 1)}{2 \cdot t_p \cdot E_s + t_{sc} \cdot E'_c} \qquad \text{(Equation 5)}$$

Where E'_c is an effective elastic concrete stiffness, S_{xy} is the unit element shear force at yield, ν_s, is Poisson's ratio for steel, E_s is the elastic modulus of steel, and t_{sc} is the SC wall thickness.

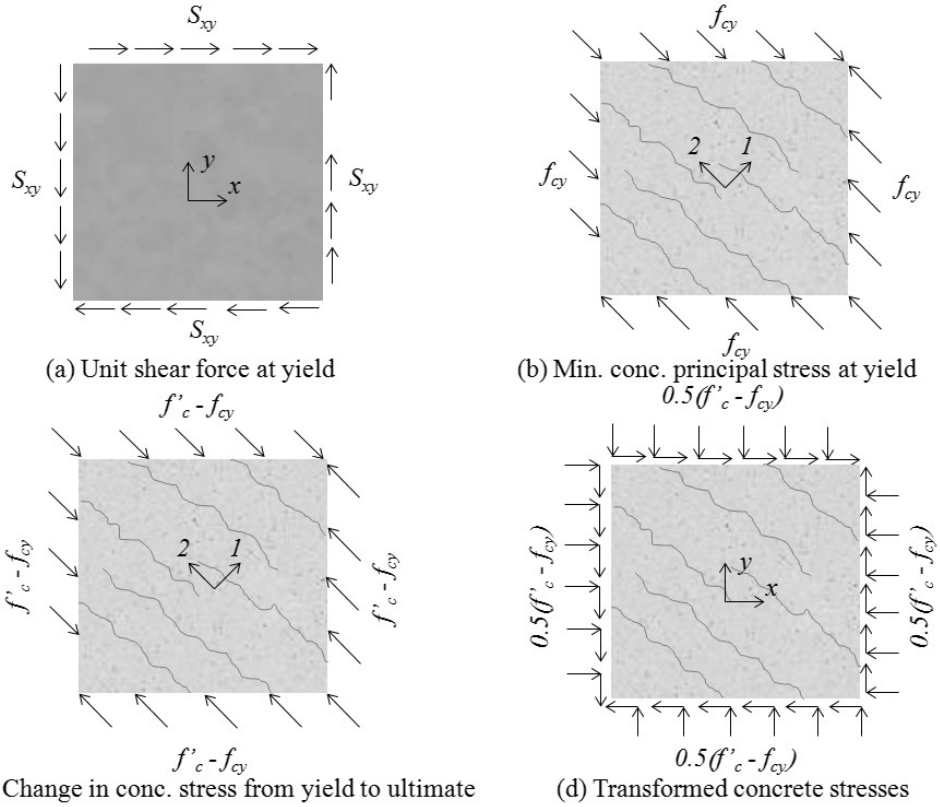

Figure 1 Shear element and concrete stresses at first yield and ultimate strength

The incremental concrete stress is then equal to $f'_c - f_{cy}$ as shown in Figure 1(c) in principal coordinates (45 degrees), and in Figure 1(d) in *x-y* coordinates. This stress is assumed to be uniform on the section of critical shear, so the incremental shear strength can be written as the incremental concrete stress multiplied by the concrete area, A_c (Equation 6). The calculated incremental shear, ΔV, is then multiplied by an empirical coefficient, *0.33*, to account for compression softening due to transverse strain and cracking, and concentration of concrete stresses due to compression strut formation.

$$\Delta V = 0.33 \cdot 0.5 \cdot (f'_c - f_{cy}) \cdot A_c \qquad \text{(Equation 6)}$$

SUMMARY OF PREVIOUS EXPERIMENTAL TESTS

Previous experimental tests have been conducted on flanged SC shear walls by Funakoshi et al. (1998), Takeuchi et al. (1998), and Fujita et al. (1998). These tests were all configured as free-standing flanged SC shear walls with the bases either embedded or mechanically connected to reinforced concrete foundations. Horizontal cyclic loads were applied to the tops of the walls such that a combination of shear and flexure were subjected to the specimens. A wide range of reinforcement ratios, ρ, and aspect ratios of the shear panels (h_w/l_w) were tested (columns 2 and 3 in Table 1). Also, the measured concrete compressive strengths and steel yield strengths are listed in columns 4 and 5, respectively.

Table 1 Summary of experimental flanged wall tests

	1	2	3	4	5	6	7	8
	Specimen	ρ (%)	h_w/l_w	f'_c (ksi)	F_y (ksi)	*Exp. Str.* (kips)	f_{cy} (ksi)	*Exp./*V_{ub}
Funakoshi et al. (1998)	BS70T05	3.9	0.56	4.7	50.2	1664	1.74	1.13
	BS50T10	2.0	0.33	5.2	55.4	1484	1.25	1.31
	BS70T10	2.0	0.56	4.7	55.4	1293	1.24	1.19
	BS85T10	2.0	0.73	4.7	55.4	1237	1.24	1.14
	BS70T14	1.4	0.56	5.2	63.8	1214	1.08	1.18
Takeuchi et al. (1998)	H07T10	2.0	0.87	4.3	41.5	927	0.92	1.10
	H10T05	4.0	1.08	4.3	41.5	549	1.57	0.81
	H10T10	2.0	1.16	4.7	41.5	815	0.93	0.93
	H10T10N	2.0	1.16	4.7	41.5	790	0.93	0.90
	H10T10V	2.0	1.16	4.7	41.5	953	0.93	1.16
	H10T15	1.3	1.26	4.3	41.5	1185	0.67	1.09
	H15T10	2.0	1.75	4.7	41.5	773	0.93	0.77
Fujita et al. (1998)	No.1	2.0	0.73	4.9	57.0	945	1.28	0.90
	No. 2	2.8	0.56	4.9	57.0	1144	1.60	0.91
	No. 3	2.8	0.56	4.9	57.0	1210	1.60	0.96
	No. 4	2.8	0.56	5.8	57.0	1210	1.63	0.90
Mean of 16 tests								1.024
Coeff. Of Variation								0.123

Column 6 in Table 1 lists the peak lateral strengths from all of the experimental tests. The calculated minimum principal concrete stress at yield, f_{cy}, is listed in column 7 and the ratio of measured experimental strength to calculated (upper bound) shear strength, V_{ub}, using (Equation 1 is listed in column 8. Overall, the calculated shear strength shows good agreement with the experimental tests, with a mean of 1.024 and a coefficient of variation of 12.3%.

ANALYTICAL MODELLING OF A SQUARE WALL STRUCTURE

A structure composed of SC walls that is square in plan is modelled with the finite element computer program Abaqus CAE (SIMULIA, 2013). The structure is modelled in 3-D with steel shell elements and solid concrete elements. The explicit solver is used so that the nonlinear geometric and inelastic material response can be simulated.

The structure is modelled as free-standing, with a fixed base, and square in plan. The analysis considers two key parameters: (1) the SC wall reinforcement ratio, ρ, and (2), the structure aspect ratio, h/L, where h is the overall height of the structure and L is the length of the structure in the direction of applied load. Three different reinforcement ratios are considered: 3.1%, 4.2% and 5.2%. The steel plate thicknesses considered and SC wall thicknesses are listed in Table 2. Five structure aspect ratios (h/L) are considered: 0.75, 1.00, 1.25, 1.50, and 1.75. The five aspect ratios combined with the three steel plate thicknesses makes for a total of 15 analytical models.

Table 2 Dimensions and properties of the wall analytical model

Plan dimensions of structure	16 ft x 16 ft
Wall thickness	24 inches
Steel plate thickness	0.375, 0.500, 0.625 (inches)
Reinforcement ratio	3.1%, 4.2%, 5.2%
Steel yield strength	55-ksi
Conc. Compressive strength	5,000-psi
Structure aspect ratios considered	0.75, 1.00, 1.25, 1.50, 1.75

In the analytical model, a concrete constitutive model is used that simulates cracking behaviour with a smeared crack approach where the tension cracking response is averaged over the element and implemented with modifications to the stiffness matrix during successive time steps. The model simulates post-cracking behaviour using the brittle fracture concept from Hillerborg et al. (1976). The constitutive model accounts for Mode I and Mode II fracture, tension softening, and shear retention. The brittle cracking model assumes linear elastic behaviour in compression in order to improve stability.

Crack initiation is determined with a Rankine failure criterion. The orientations of crack surfaces are defined at initial cracking and fixed to the local coordinates of the element for the duration of the analysis. Cracking is possible on three planes on a given element. When the first crack initiates, the orientation is fixed and potential cracking in the remaining two directions occur on perpendicular planes. The post-cracking response (tension stress-crack opening displacement and shear retention) is implemented with recommended parameters from the CEB-FIP Model Code for Concrete Structure (1990).

The composite behaviour of the SC section is modelled with nonlinear connector elements that are each assigned a force-slip curve based on the formulation by Ollgaard et al. (1971). The connectors tie coincident nodes on the surface of the concrete solids to nodes on the steel shell elements. Each of the coincident nodes are assigned a local coordinate system with the x and y-directions located in the slip plane parallel to the surface of the concrete and the z-direction perpendicular to the surface.

The model parts and meshing are shown in Figure 2. The corners of the wall structure are detailed with boxed sections that partition the concrete infill into 8 separate parts: four concrete extrusions that fill the corners, and four wall infill parts. The boundary condition at the base of the structure is fixed and a lateral load is applied to the upper (elastic) loading block. The results of the pushover analyses are plotted (for aspect ratios of 0.75, 1.00, 1.25, 1.50) in Figure 3. The plots show the overturning moment response

(lateral load multiplied by height of structure) vs. horizontal displacement of the top of the structure for the three different reinforcement ratios).

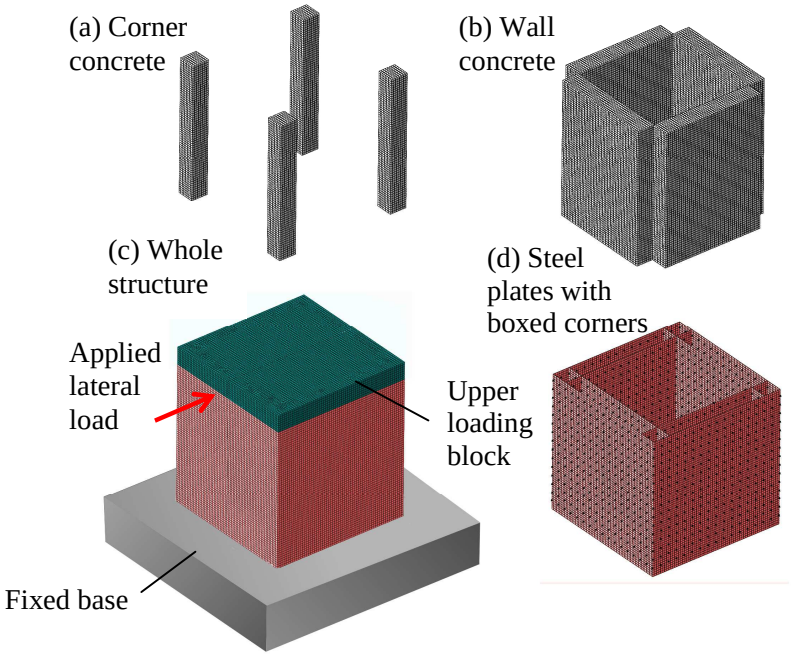

Figure 2 (a) Corner concrete, (b) wall concrete, (c) whole structure (d), steel plates with boxed corners

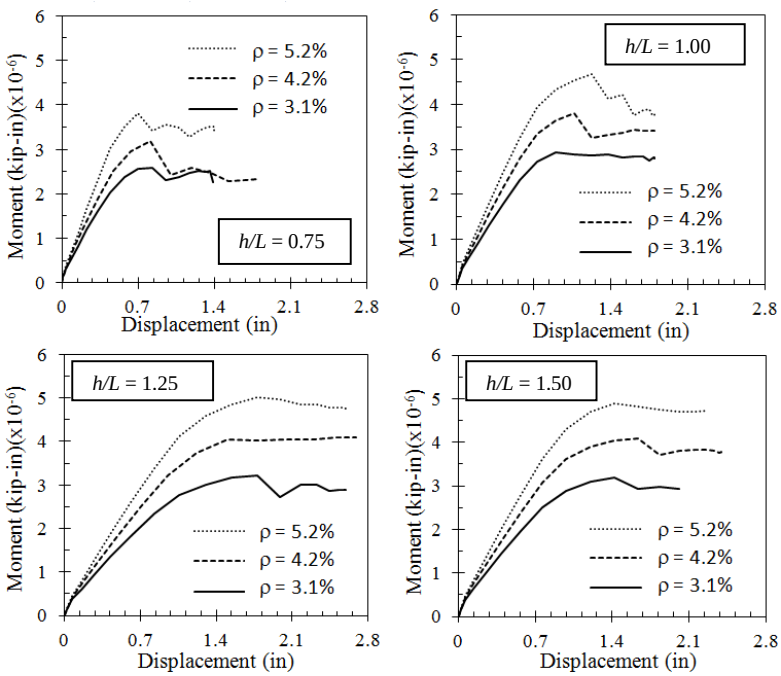

Figure 3 Load displacement results from analytical wall structure with four different aspect ratios and three different reinforcement ratios

As shown, the overturning strength of the h/L = 0.75 structures is less than for the taller three structures since failure of these structures is initiated by shear failure of the SC walls before the full flexural strength

of the structure is reached. The overturning strengths of the 1.00 and 1.25 aspect ratio structures are very similar although the 1.25 aspect ratio structure exhibits slightly more ductility.

DESIGN RECOMMENDATIONS

Shear Strength

Three calculated shear strengths are considered: (a) the in-plane shear defined at steel yielding (V_y), (b), the calculated upper bound shear strength, V_{ub}, and (c), the out-of-plane shear strength (V_{oop}). Using these shear strengths, the strength of the structure at yield of the shear walls, and the upper bound strength of the structure are calculated. For yield, the shear strength is equal to V_y of the web walls plus V_{oop} of the flange walls. Similarly, for the upper bound shear strength, the total shear is equal to V_{ub} plus V_{oop}.

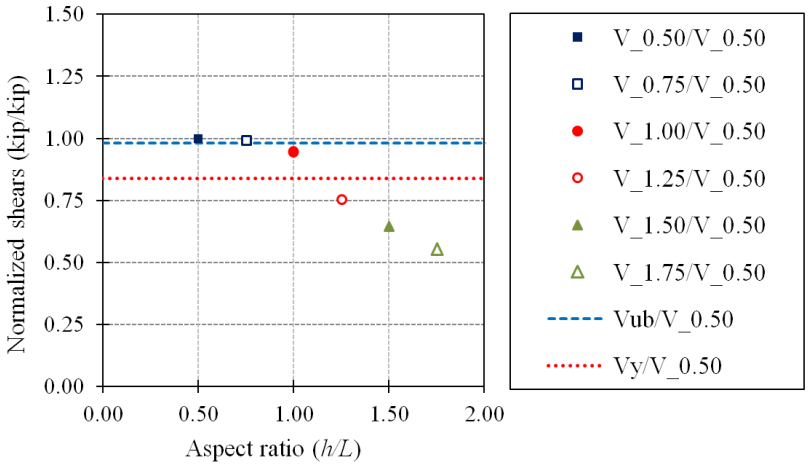

Figure 4 Calculated and finite element results of structure strength for the octagonal structure

The out-of-plane shear strength is assumed to be equal to $3\sqrt{f'_c}$ (with psi units) multiplied by the gross concrete area of the two flange walls. Figure 4 plots the peak shear forces in the web walls from the finite element analyses of the structure with the 5.2% reinforcement ratio walls. The values shown are taken at the point of ultimate strength of the structure for the 6 aspect ratios (V_0.50, V_0.75, V_1.00, V_1.25, V_1.50, and V_1.75). In the figure, the shear forces are normalized by the shear force, V_0.50. Also shown, are the calculated shears, V_{ub} and V_y (also normalized with respect to V_0.50). As shown, the strengths increase at lower aspect ratios and appear to level off as the aspect ratio approaches 0.50. The normalized calculated strengths, V_y and V_{ub}, are also plotted. As shown the upper bound shear in plane shear strength, V_{ub}, shows improved agreement with the analyses as the aspect ratio approaches 0.50.

Flexural Strength

The structure aspect ratio has a significant effect on the overall response of the structure and governing failure modes. For a given structure with identical cross-sectional properties and varying structure height, the peak lateral strength will either be governed by flexure for taller structures or a combination of flexure and shear for shorter structures. In Figure 5 and Figure 6, peak strengths of the 15 analyzed structures are shown. The peak overturning strengths are plotted vs. aspect ratio. For structure heights greater than approximately 1.0, the overturning strengths of the structures plateau as the responses become controlled by the flexural strengths of the sections. Also, a slight reduction in ultimate strength is apparent at the shear-flexure transition point due to shear-flexure interaction.

The flexural strength of the structure is calculated with a rigid-plastic fibre model analysis as defined in AISC N690-12s1. The model assumes that the steel on the flexural section is all at yield (fully plastic) and that the concrete on the compression side of the neutral axis is in uniform compression and equal to $0.85f'_c$. It is also assumed for simplicity that the concrete cannot resist flexural tension stress, consequently, all of the concrete below the neutral axis is considered "fully cracked".

Strength of Structure

The ultimate overturning strength of the square wall structure is calculated as the lesser of the shear strength multiplied by the structure height or the flexural strength of the section. In both Figure 5 and Figure 6 the previously described calculation for flexural strengths are plotted (horizontal solid lines). The results show that the analytical and fibre model flexural strengths show good agreement for the 1.50 and 1.75 aspect ratio analyses.

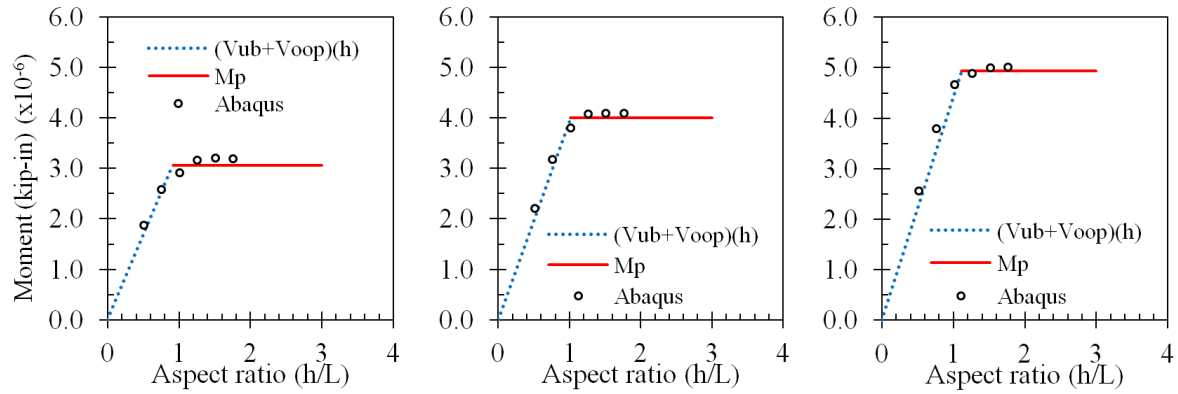

Figure 5 Calculated and analytical strength of square wall structure using V_{ub} as the design shear strength

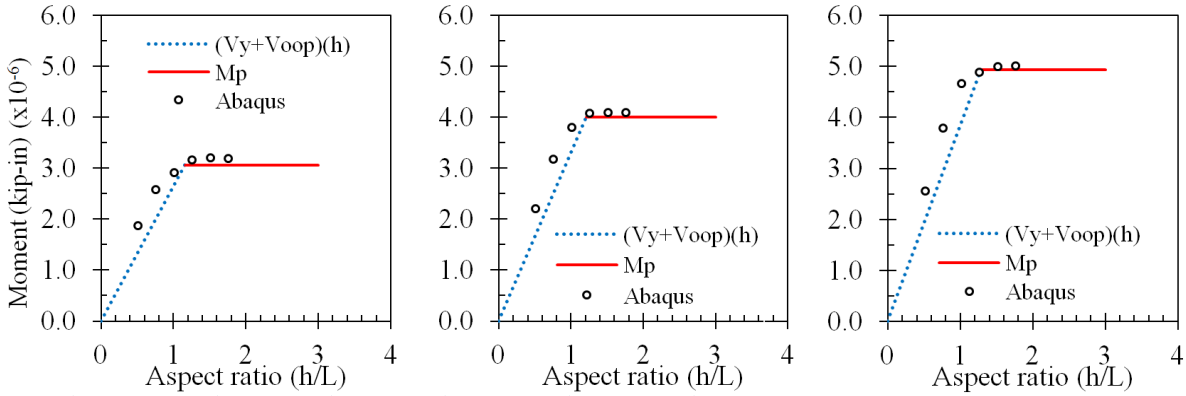

Figure 6 Calculated and analytical strength of the square wall structures using V_y as the design shear strength

The calculated shear strengths are also shown in Figure 5 and Figure 6. For aspect ratios less than approximately 1.0, the strengths are assumed to be controlled by shear. In Figure 5, the shear critical leg (dotted lines) are defined as the sum of the upper bound shear strength and the out-of-plane shear strength multiplied by the structure height, *h*. Similarly in Figure 6, the shear strength legs are defined as the sum of the shear yield strength V_y, and the out-of-plane shear strength multiplied by the structure height. The results show that the strength envelopes shown in Figure 5 provide a good prediction of the ultimate overturning strength of structure for the given reinforcement ratios of 3.1%, 4.2% and 5.2%, although the predictions are slightly unconservative at the shear-flexure transition points. In contrast, the strength

envelopes shown in Figure 6 that use $V_y + V_{oop}$ instead of $V_{ub} + V_{oop}$, appear slightly conservative for aspect ratios below approximately 1.0.

SUMMARY AND CONCLUSIONS

A method is presented for calculating the ultimate overturning strength of an SC wall structure that is square in plan. The strength is assumed to be the lesser of the flexural strength of the structure and the calculated shear strength considering both out-of-plane and in-plane shear. The in-plane shear strength is calculated with an approach based on composite shell theory and takes into account reserve shear strength that can occur in shear walls with boundary elements. This approach predicts additional shear strength beyond the point of steel yield in the shear wall resulting from diagonal compression in the concrete infill. Arch action occurring from diagonal concrete compression struts are resolved as vertical tension in the perpendicular flange walls of the structure. For the flexural strength, a rigid-plastic fibre model is developed that considers (i) all of the steel on the section to be yielded, (ii) the concrete stress on the compression side of the neutral axis equal to $0.85f'c$, and (iii) zero concrete tension stresses.

The calculated shear strengths are compared with an experimental database including 16 tests of flanged shear walls in the literature. The calculated shear strengths show good agreement with the database with a mean of 1.024 and a coefficient of variation of 12.3%.

The finite element modelling approach is used to develop detailed 3-D models of 15 square SC wall structures of varying aspect ratios (h/L) and reinforcement ratios. The calculated shear and flexural strengths are then compared to the analytical results. The comparisons show very good agreement between the fibre model based flexural strengths and the analyses at higher aspect ratios (1.50 and 1.75). For the shear strengths, the strength calculation using V_{ub} is shown to predict the ultimate strength although also slightly unconservative for aspect ratios at the shear-flexure control transition points. Also, the shear strength calculation using the shear yield strength, V_y, is shown to be conservative for structural aspect ratios below approximately 1.0.

REFERENCES

AISC N690-12s1, Specification for safety-related steel structures for nuclear facilities, suppl. no. 1, Public review draft, AISC, Chicago, IL, 2014.

CEB-FIP Model Code 1990. Thomas Telford Services Ltd., London.

Cummins, W. E., (2001), *The Advanced Passive AP1000 Nuclear Plant - Competitive and Environmentally Friendly*, Transactions of the 16th International Conference on Structural Mechanics in Reactor Technology, Washington DC, USA.

Fujita, T., A. Funakoshi, S. Akita, I. Matsuo (1998). "Experimental Study on a Concrete Filled Steel Structure Part 14 thru 17 Bending Shear Tests," Summaries of Technical Papers of Annual Meeting, Arch. Inst. of Japan, pp. 1121-1128.

Funakoshi, A., Akita, S., Matsumoto, H., Hara, K., Matsuo, I., and Hayashi, N. (1998) Experimental study on a concrete filled steel structure Part. 7 Bending Shear Tests (Outline of the experimental program and the results), Summaries of Technical Papers of Annual Meeting, Architectural Institute of Japan, pp. 1063-1064.

Hillerborg, A., Modeer, M., Petersson, P. E., (1976). "Analysis of Crack Formation and Crack Growth in Concrete by Means of Fracture Mechanics and Finite Elements," Cement and Concrete Research, Vol. 6, pp. 773-782.

Ollgaard, J. G., Slutter, R. G., and Fisher, J. W. (1971). "Shear strength of stud connectors in lightweight and normal weight concrete," AISC Engineering Journal, Fritz Laboratory Reports.

SIMULIA Dassault Systems (2013). ABAQUS Analysis User's Manual.

Takeuchi, M., Narikawa, M., Matsuo, I., Hara, K., Usami, S. (1998). "Study on a concrete filled structure

for nuclear power plants," Nuclear Engineering and Design," Nuclear Engineering and Design, Vol. 179, Issue 2, pp. 209–223.

Varma, A. H., Zhang, K., Chi, H., Booth, P., Baker, T. (2011). In-plane shear behaviour of SC composite walls: theory vs. Experiment, Transactions, SMiRT 21, New Delhi, India.

Varma, A. H., Malushte S. R., Sener, K. C., and Lai, Z. (2014). "Steel-Plate Composite (SC) Walls for Safety Related Nuclear Facilities: Design for In-Plane Force and Out-of-Plane Moments," Nuclear Eng. and Design. Special Issue on SMiRT-21 Conference. Vol. 269, pp: 240-249.